The impact of the 2016 Fort McMurray Horse River Wildfire on ambient air pollution levels in the Athabasca Oil Sands Region, Alberta, Canada

Matthew S. Landis [a,*], Eric S. Edgerton [b], Emily M. White [c], Gregory R. Wentworth [d], Amy P. Sullivan [e], Ann M. Dillner [f]

[a] US EPA, Office of Research and Development, Research Triangle Park, NC, USA
[b] Atmospheric Research & Analysis, Inc., Cary, NC, USA
[c] Maed Consulting, Chapel Hill, NC, USA
[d] Alberta Environment and Parks, Environmental Monitoring and Science Division, Edmonton, AB, Canada
[e] Colorado State University, Fort Collins, CO, USA
[f] University of California, Davis, CA, USA

HIGHLIGHTS

- Horse River Fire had a major air quality impact on the city of Fort McMurray.
- $PM_{2.5}$ enhancements at the community monitoring sites ranged from a factor of 19–54.
- Significant enhancements of NMHC, NH_3, BC, DC, TRS, NOx, and H_2S were observed.
- First observations of reduced sulfur compounds (TRS/H_2S) emissions from a wildfire
- Fire $PM_{2.5}$ profiles were uniform across the network, can be used as a fingerprint.

GRAPHICAL ABSTRACT
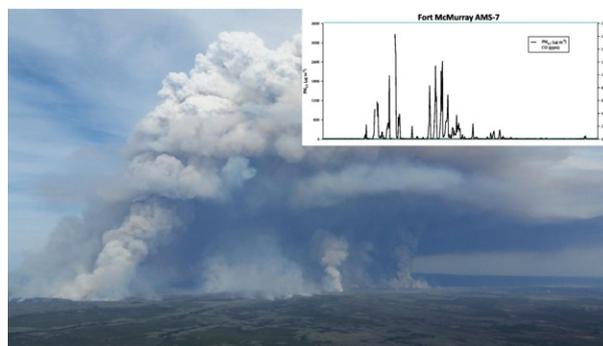
ARTICLE INFO

ABSTRACT

An unprecedented wildfire impacted the northern Alberta city of Fort McMurray in May 2016 causing a mandatory city wide evacuation and the loss of 2,400 homes and commercial structures. A two-hectare wildfire was discovered on May 1, grew to ~157,000 ha by May 5, and continued to burn an estimated ~590,000 ha by June 13. A comprehensive air monitoring network operated by the Wood Buffalo Environmental Association (WBEA) in and around Fort McMurray provided essential health-related real-time air quality data to firefighters during the emergency, and provided a rare opportunity to elucidate the impact of gaseous and particulate matter emissions on near-field communities and regional air pollution concentrations. The WBEA network recorded 188 fire-related exceedances of 1-hr and 24-hr Alberta Ambient Air Quality Objectives. Two air monitoring sites within Fort McMurray recorded mean/maximum 1-hr $PM_{2.5}$ concentrations of 291/5229 $\mu g\,m^{-3}$ (AMS-6) and 293/3259 $\mu g\,m^{-3}$ (AMS-7) during fire impact periods. High correlations ($r^2 = 0.83$–0.97) between biomass combustion related gases (carbon monoxide (CO), non-methane hydrocarbons (NMHC), total hydrocarbons (THC), total reduced sulfur (TRS), ammonia) and $PM_{2.5}$ were observed at the sites. Filter-based 24-hr integrated $PM_{2.5}$ samples collected every 6 days showed maximum concentrations of 267 $\mu g\,m^{-3}$ (AMS-6) and 394 $\mu g\,m^{-3}$ (AMS-7). Normalized excess emission ratios relative to CO were 149.87 $\pm$ 3.37 $\mu g\,m^{-3}\,ppm^{-1}$ ($PM_{2.5}$), 0.274 $\pm$ 0.002 ppm ppm^{-1} (THC), 0.169 $\pm$ 0.001 ppm ppm^{-1} (NMHC), 0.104 $\pm$ 0.001 ppm ppm^{-1} (CH_4), 0.694 $\pm$ 0.007 ppb ppm^{-1} (TRS), 0.519 $\pm$ 0.040 ppb ppm^{-1} (SO_2), 0.412 $\pm$ 0.045 ppb ppm^{-1} (NO), 1.968 $\pm$

* Corresponding author.
  E-mail address: landis.matthew@epa.gov (M.S. Landis).

0.053 ppb ppm^{-1} (NO$_2$), and 2.337 ± 0.077 ppb ppm^{-1} (NO$_x$). A subset of PM$_{2.5}$ filter samples was analyzed for trace elements, major ions, organic carbon, elemental carbon, and carbohydrates. Sample mass reconstruction and fire specific emission profiles are presented and discussed. Potential fire-related photometric ozone instrument positive interferences were observed and were positively correlated with NO and NMHC.

1. Introduction

Over the last thirty-four years (1983–2016) the number of wildfires in the United States has not significantly changed (Appendix A.1a), while the total acreage burned has significantly (Appendix A.1b) increased (United States National Interagency Fire Center, 2017). Nine of the ten highest acreage burn years have occurred since 2000, including the peak of 4.1 million ha in 2015. This time period coincides with many of the warmest years on record in the United States (United States Environmental Protection Agency, 2016). The combination of increased temperature, drought, earlier snowmelt, and historically high fuel loading (e.g., undergrowth and tree density) generally promotes more aggressive fire behavior (Kitzberger et al., 2007; Littell et al., 2009; United States Department of Agriculture, 2014; United States Department of Agriculture, 2016; Westerling, 2016). In addition to increasing size, the intensity of fires estimated as both moderate (Appendix A.2a) or severe (Appendix A.2b) damage have significantly increased from 1984 to 2014 (United States Wildland Fire Leadership Council, 2016; Miller et al., 2009). In Canada over the last fifty-five years (1961–2015) both the number of fires (Appendix A.3a) and the total acreage burned have significantly (Appendix A.3b) increased (Stocks et al., 2003; Canadian Forest Service, 2016). However, the number of fires in Canada has leveled off over the last two decades (Appendix A.3a). In the Province of Alberta, the number of wildfires has steadily increased (Appendix A.4a) throughout the time period and peaked at 1954 fires in 2006 (Alberta Agriculture and Forestry, 2017). The trend in acreage burned in Alberta is generally stable with typical annual totals < 100,000 ha, punctuated by periodic large catastrophic fires (Appendix A.4b) like the 2011 Richardson Backcountry fire that consumed > 577,000 ha in the north-eastern portion of the Province (Liu et al., 2015).

Smoke from wildland fire is an increasing global public health research focus as information on the relative magnitude of atmospheric emissions and the resulting human health effects are elucidated. The combined contribution from wildland and agricultural fires to the emission of U.S. primary air pollutants such as black carbon (BC), fine particulate matter (PM$_{2.5}$; median aerodynamic diameter < 2.5 μm), carbon monoxide (CO), and volatile organic compounds (VOCs) constitute 43%, 34%, 32%, and 29% of the annual total in the 2011 national emission inventory (NEI), respectively (United States Environmental Protection Agency, 2015). In addition, wildland fire emissions contribute to the formation of photochemically mediated secondary organic aerosol (Donahue et al., 2009; Ortega et al., 2013; Baker et al., 2016). Wildfire smoke has been shown to have detrimental respiratory and cardiovascular health effects, is associated with all-cause mortality and morbidity, and exhibits lung toxicity and mutagenicity ~60 times greater than diesel exhaust (Lee et al., 2014; Liu et al., 2015; Reid et al., 2016; Adetona et al., 2016; Kim et al., 2017). Smoke from wildfires in Alberta, Saskatchewan, and the Northwest Territories has been shown to affect air pollution concentrations in communities in the Athabasca Oil Sands Region (AOSR) in Alberta, Canada (Bytnerowicz et al., 2016; Landis et al., 2017). The Wood Buffalo Environmental Association (WBEA) Bertha Ganter-Fort McKay community air monitoring site (AMS-1) PM$_{2.5}$ monthly geometric mean concentrations reflect clearly observable wildfire smoke impacts during the summers of 2011, 2012, 2014, and 2015 (Percy, 2013; Appendix A.5a). Similar wildfire smoke impact trends are observable at the AMS-6 and AMS-7 community monitoring sites in the region (Appendix A.5b–c).

In May 2016 an unprecedented wildfire (Horse River Fire) impacted the northern Alberta city of Fort McMurray in the AOSR, causing a mandatory evacuation of all residents and the loss of over 2400 homes and commercial structures. Weather conditions preceding the fire were unseasonably hot (daily highs up to 35 °C), windy (sustained 10 m winds reaching 43 km hr^{-1}), and the region was experiencing an El Nino influenced drought. An estimated two-hectare wildfire was first discovered on May 1 by a fire patrol and despite an immediate response quickly jumped the Athabasca River, burned through the northern portion of the city, and grew to ~157,000 ha over the next four days. The fire continued to burn through June 13, 2016 with an estimated total size of ~590,000 ha (Fig. 1), resulting in $3.6 billion (CAD) of insured losses. The community air monitoring network operated by WBEA in and around Fort McMurray operated continuously throughout the fire event and recorded 188 exceedances of 1-hr and 24-hr Alberta Ambient Air Quality Objectives (AAAQOs) for PM$_{2.5}$, hydrogen sulfide (H$_2$S), ozone (O$_3$), nitrogen dioxide (NO$_2$), and CO during the event in May 2016 (Government of Alberta, 2017; Appendix B.1). The progression of the Horse River Fire through the comprehensively instrumented air monitoring network provided a rare opportunity to elucidate the impact of gaseous and particulate matter emissions on near-field and regional communities' air pollution concentrations in the vicinity of a northern boreal forest mega fire (Appendix A.6a–b). Canada contains 28% of the worlds boreal zone area (552 million ha), and 75% of Canadian forests and woodlands (307 million ha) are located in the boreal zone (Natural Resources Canada, 2017). The two predominant tree species in the AOSR are Jack Pine (*Pinus banksiana*) and Black Spruce (*Picea mariana*).

This study's goals were to (i) quantify the relative enhancement of ambient air pollution concentrations due to smoke from the Horse River Fire in surrounding AOSR communities, (ii) calculate emission ratios of fire related pollutants of human and ecological concern, (iii) chemically characterize measured PM$_{2.5}$ and PM$_{10}$ constituents, and (iv) summarize reconstructed PM$_{2.5}$ mass.

2. Methods

2.1. WBEA monitoring network

At the time of the fire, WBEA operated a continuous ambient air monitoring network in the AOSR comprised of six community monitoring sites, eleven industrial monitoring sites, one regional background monitoring site, one comprehensive meteorological site, and one mobile monitoring site covering an area ~350 km (N-S) and ~125 km (E-W; Fig. 1; Appendix B.2). The AMS-6 Patricia McInnes-Fort McMurray (56°45′5.00″ N; −111°28′35.75″ W), AMS-7 Athabasca Valley-Fort McMurray (56°44′0.18″ N; −111°23′25.75″ W), and AMS-14 Anzac (56°26′56.19″ N; −111°2′16.84″ W) community ambient air monitoring stations were located within the Horse River Fire burn area (Fig. 1). The fire burn area was bounded to the north by the AMS-1 Bertha Ganter-Fort McKay community site (57°11′21.70″ N; −111°38′26.06″ W) and to the south by the AMS-18 Stony Mountain regional background site (55°37′17.19″ N; −111°10′22.16″ W). The community AMS stations provide near real-time ambient air quality information, including the Air Quality Health Index (AQHI), to their respective populations.

WBEA was also operating a network of ecologically analogous jack pine stand level Forest Health Monitoring sites measuring monthly
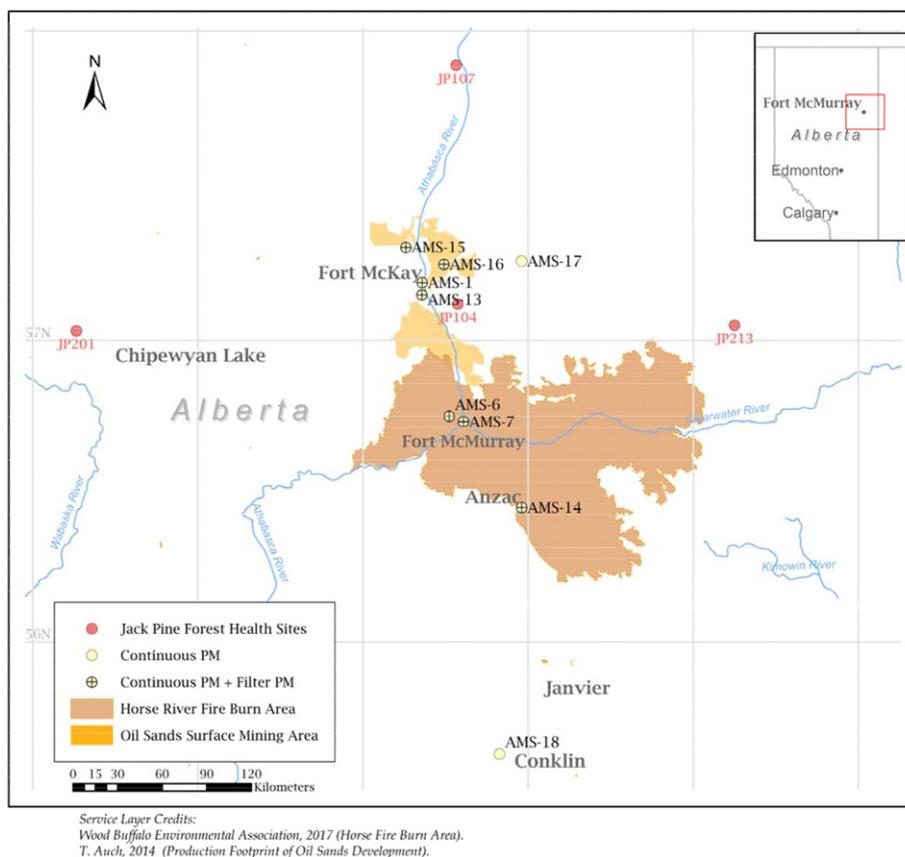
Fig. 1. Map depicting the location of the WBEA air monitoring sites measuring continuous PM$_{2.5}$, the outline of the Horse River Fire burn area, and the outline of oil sand surface mining area.

integrated ambient concentrations of sulfur dioxide (SO$_2$), NO$_2$, O$_3$, ammonia (NH$_3$), and nitric acid (HNO$_3$) via passive sampling (Percy, 2013). The purpose of this remote helicopter-only accessible network is to estimate ecosystem exposures to regional air pollutants, at distances up to 150 km from mining and upgrading operations.

2.2. Study design

The continuous measurement study period was defined as April 1–July 31, 2016; which includes approximately a month both before and after the Horse River Fire. The quality assured 5-min and 1-hr integrated monitoring data from all the WBEA ambient monitoring stations (AMS) measuring continuous PM$_{2.5}$ concentrations (AMS-1, AMS-6, AMS-7, AMS-13, AMS-14, AMS-15, AMS-16, AMS-17, AMS-18, AMS-21) were included in the study (Wood Buffalo Environmental Association (WBEA), 2016). Continuous monitoring data from the AMS-14 site was interrupted from May 6–14 due to power being turned off to the site as a fire precaution, and continuous PM$_{2.5}$ measurements were interrupted at AMS-21 from May 5–11 as a result of a pump failure following a short power interruption. The filter based measurement study period was defined as April 1–August 4, 2017 to allow for an additional sampling day to be included to characterize non-fire conditions.

2.3. WBEA AMS continuous measurements

Routine WBEA ambient monitoring data includes continuous (i) PM$_{2.5}$ mass measured using ThermoScientific (Franklin, MA) Model 5030 Synchronized Hybrid Ambient Real-time Particulate Monitors (SHARP), (ii) nitrogen oxide (NO), NO$_2$, and total oxides of nitrogen (NOx) measured using ThermoScientific Model 42i and Teledyne API (San Diego, CA) Model T200 chemiluminescence analyzers, (iii) SO$_2$ measured using ThermoScientific Model 43i and Teledyne API Model

T100 pulsed fluorescence analyzers, (iv) NH$_3$ measured using ThermoScientific Model 17i and Teledyne API Model T201 chemiluminescence analyzers, (v) CO measured using a ThermoScientific Model 48i gas filter correlation analyzer, (vi) O$_3$ measured using ThermoScientific Model 49i and API Model T400 UV absorption analyzers, (vii) H$_2$S measured using ThermoScientific Model 450i and API Model T101 UV fluorescence analyzers, (viii) Total Hydrocarbons (THC) measured using ThermoScientific Model 51i flame ionization detector (FID) instruments, (ix) Non-methane Hydrocarbons (NMHC) and methane (CH$_4$) measured using ThermoScientific Model 55i gas chromatography FID instruments, and (x) total reduced sulfur (TRS) measured using ThermoScientific Model 43i coupled with a CD Nova Ltd. (Surrey, BC) Model CDN101 high temperature thermal oxidizer (Wood Buffalo Environmental Association (WBEA), 2016). All continuous gas analyzers in the WBEA monitoring network are automatically single point span calibrated and zeroed on a daily basis using Teledyne API Model T700 dynamic dilution calibration systems with U.S. EPA protocol certified gas standards. Multi-point span calibrations are conducted on a monthly basis. The SHARP PM$_{2.5}$ instruments beta gauges are calibrated with certified mass foil sets every six months and the instruments nephelometers are zeroed on a monthly basis.

2.4. WBEA AMS filter based particulate matter measurements

Routine 24-hr integrated filter based measurements of PM$_{2.5}$ (sites AMS-1, AMS-6, AMS-7, and AMS-14) and PM$_{10}$ (sites AMS-1, AMS-6, AMS-7, AMS-13, AMS-14, AMS-15, and AMS-16) are carried out using collocated ThermoScientific Model 2000i Partisol U.S. EPA designated Federal Reference Method (FRM) samplers. Measurement Technologies Laboratories (Minneapolis, MN) 47 mm Teflon membrane filters with Teflon support rings samples are robotically weighed for PM$_{2.5}$ and PM$_{10}$ mass by Atmospheric Research & Analysis, Inc. (ARA, Morrisville,

NC) using a method described by Landis et al. (2017). One of each collocated filter pair is extracted and analyzed for major ions, and the other collocated filter is extracted and analyzed for trace elements as described below. Bracketing the Horse River Fire, a subset of the Teflon filter samples was selected for additional carbohydrate and organic carbon (OC)/elemental carbon (EC) analysis. At the AMS-1 site, an additional 24-hr integrated $PM_{2.5}$ sample is routinely collected onto a quartz filter for determination of OC/EC. Filter samples are collected according to the Canadian National Air Pollution Surveillance Program (NAPS) 1-in-6-day schedule.

2.5. WBEA forest health monitoring site measurements

WBEA collects tower-based annular denuder samples at four forest health sites (JP104, JP107, JP201 and JP213) to obtain above-canopy measurements of HNO_3 and NH_3 across the AOSR. JP104 is located approximately 45 km N of Fort McMurray and 25 km SSE of Fort McKay, and JP201, JP107 and JP213 are located 100–150 km W, N and E of JP104, respectively (Fig. 1). Samples are collected at a height of ~25 m above ground level (roughly 5 m above canopy; Appendix A.7a) using solar-power for flow maintenance and data logging, and two URG Corporation (Carrboro, NC) 150 mm multi-channel annular denuders (URG-2000-30x150-3CSS) in series coated with potassium chloride (KCl) and citric acid for capture of HNO_3 and NH_3, respectively (United States Environmental Protection Agency, 1999a, 1999b). Samples are collected over nominal monthly intervals at a flow rate of 1.25 L min^{-1}. Following exposure, denuders are sealed and returned to the ARA laboratory for analysis. Field blanks are collected with each monthly deployment and used to blank-correct each batch of samples. One of the samplers at JP104 is configured for the collection of $PM_{2.5}$. This sampler has an in-line $PM_{2.5}$ cut point cyclone downstream of the KCl and citric acid denuders followed by a two-stage filter pack containing a Teflon pre-filter and a nylon backup filter (Appendix A.7b). The Teflon filter captures non-volatile $PM_{2.5}$ while the nylon filter captures volatile nitrate lost from the Teflon filter during sampling. After exposure, filter packs are sealed and returned to the ARA laboratory for extraction and analysis. Teflon filters are weighed and then cut in half, with one half used for analysis of major ions and the other half used for trace element analysis.

2.6. Carbon analysis

Quartz filter samples collected at the AMS-1 Fort McKay site were analyzed for OC and EC by Desert Research Institute (Reno, NV) using both the thermal optical transmission (TOT) NIOSH method 5040 (United Stated National Institute for Occupational Safety and Health, Manual of Analytical Methods (NMAM), et al., 2003) and thermal optical reflectance (TOR) IMPROVE_A protocol (Chow et al., 1993; Chow et al., 2007). Routine semi-continuous (5-min) BC measurements were made using Magee Scientific (Berkeley, CA) model AE-33 spectrum Aethalometers (Drinovec et al., 2015) at the AMS-1 and AMS-18 sites. Organic components of biomass combustion emissions have been observed to result in enhanced UV (370 nm) relative to IR (880 nm) wavelength optical absorption, the enhanced absorption is expressed as Delta-C (DC) in units of $\mu g\ m^{-3}$, and calculated as BC_{370}–BC_{880} (Allen et al., 2004).

2.7. Fourier transform infrared spectrometer analysis for OC and EC

A subset of the routinely collected AMS $PM_{2.5}$ FRM samples was also analyzed using a Bruker Optics (Billerica, MA) Model Tensor II Fourier transform infrared (FTIR) spectrometer equipped with a liquid nitrogen-cooled wide-band mercury cadmium telluride detector. TOR equivalent OC and EC measurements (Chow et al., 2007) are obtained from the FTIR spectra via a partial least squares regression calibration.

Complete method details can be found elsewhere (Weakley et al., 2016).

2.8. Filter extraction and trace element analysis

Following filter post weighing, the primary set of the $PM_{2.5}$ and PM_{10} sample filters were microwave digested in an acid-peroxide solution and analyzed for 43 elements using a Perkin-Elmer (Waltham, MA) Model 9000 Elan-II dynamic reaction cell inductively coupled plasma mass spectrometer (DRC-ICPMS) by ARA using a method described by Landis et al. (2017). Instrument drift and suppression, or enhancement of instrument response caused by the sample matrix, was corrected by internal standardization (Edgerton et al., 2012). Target isotopes and method detection limits (MDLs) are presented in Landis et al. (2017).

2.9. Major ions

Following filter post weighing, the collocated set of $PM_{2.5}$ and PM_{10} sample filters were extracted with 30 mL of ASTM Type I (18.2 M$\Omega \cdot$cm) ultra-pure water and analyzed for major ions (Cl^-, F^-, NO_3^-, SO_4^{2-}, PO_4^{3-}, NH_4^+, Ca^{2+}, Mg^{2+}, K^+, Na^+) using ion chromatography (IC) (United States Environmental Protection Agency, 1997). Forest health tower annular denuders were extracted with 10 mL of ASTM Type I ultra-pure water and analyzed for major ions (NO_3^-, SO_4^{2-}, NH_4^+) using IC. A Dionex (Sunnyvale, CA) Model ICS-3000 dual channel instrument equipped with a Dionex Model AS40 autosampler was utilized. Ion separations were performed with a 100 μL sample loop injection onto a Dionex IonPac© AS18 analytical column (anions) and a 25 μL sample loop injection onto a Dionex IonPac© CS16 analytical column (cations). Each channel operates a Dionex self-regenerating SRS-ULTRA suppressor in external regeneration mode, a CD20 conductivity detector, and a GP50 gradient pump with built-in degassing. The system uses Dionex eluent cartridges and laboratory-produced ASTM Type I ultra-pure water for automated generation of eluents: potassium hydroxide for anions and methanesulfonic acid for cations. The IC system was calibrated with NIST-traceable mixed standard solutions with concentrations of each analyte in the range of 0.05–5.0 mg L^{-1}. Following calibration of the IC, independent quality control solutions were analyzed to confirm accuracy. Multiple secondary source standards are also used to routinely assess precision and accuracy.

2.10. Carbohydrates

A subset of the AMS $PM_{2.5}$ and PM_{10} FRM sample aqueous extracts during the study period was also analyzed for levoglucosan, mannosan, galactosan, and other carbohydrate smoke markers. The carbohydrate smoke markers were determined using high-performance anion-exchange chromatography-pulsed amperometric detection (HPAEC-PAD) using a Dionex DX-500 series ion chromatograph with a Dionex CarboPac PA-1 column (4 × 250 mm) employing a sodium hydroxide gradient. Full details of the method can be found in Sullivan et al. (2011a, 2011b, 2014).

2.11. Statistical analysis

Data processing and all statistical analyses were performed using SAS v.9.4 (SAS Institute, Cary, NC). Parametric statistics used in this analysis included a *t*-test for independent samples, and one-way analysis of variance (ANOVA). The assumptions of the parametric procedures were examined using residual plots, skewness and kurtosis coefficients, Shapiro-Wilk test, and the Brown-Forsythe test. If assumptions of the parametric procedures were violated, then the Wilcoxon and Kruskal-Wallis non-parametric procedures were used. One-sided tests and a level of significance of $\alpha = 0.05$ were used for all statistical procedures unless otherwise stated. The SAS REG and ORTHOREG procedures were used for least square general linear model regressions.

3. Results and discussion

3.1. Impact of fire emissions on hourly average air pollution concentrations

In the past, researchers have used a fixed $PM_{2.5}$ concentration cut off of 25 µg m^{-3} in the AOSR (Bytnerowicz et al., 2016) and in Finland (Saarnio et al., 2010) to categorize fire impacted sampling periods due to smoke from boreal forest wildfires. In this case, the proximity of the Horse River Fire to the WBEA ambient monitoring network sites, the high time resolution air quality measurements, and the magnitude of impact provided the opportunity to definitively delineate the smoke impact events. Hourly integrated WBEA continuous data were categorized as fire impacted during the study period if $PM_{2.5}$ concentrations were elevated relative to pre-fire concentrations and were coincident with multiple elevated indicators of biomass combustion such as CO, NMHC, THC, TRS, H_2S, and NH_3. Fig. 2 presents a time series of $PM_{2.5}$, CO, NMHC, and TRS at the AMS-7 Athabasca Valley community monitoring site during the study period highlighting the Horse River Fire impact periods. Similar time series plots are presented for the other AMS sites in Appendix A.8a–i. The AMS-7 community site was located within the fire burn area and was the only AMS site monitoring CO, which is considered a good near-field indicator of wildland fire emissions (Urbanski, 2013). Ten exceedances of the hourly AAAQO for CO (13 ppm) were recorded at the AMS-7 site during the Horse River Fire (Appendix B.1). During the study period, CO concentrations at AMS-7 had significant ($p < 0.0001$) positive correlations with $PM_{2.5}$ (0.91), THC (0.99), NMHC (0.99), CH_4 (0.97), TRS (0.97), and NO_2 (0.77) demonstrating the efficacy of their use in conjunction with $PM_{2.5}$ as indicators of biomass combustion impact at other sites not measuring CO.

A statistical summary of the AMS site fire impacted and non-impacted hourly integrated continuous data are presented in Table 1.

There is no regulatory AAAQO for 1-hr $PM_{2.5}$, but the non-regulatory Alberta Ambient Air Quality Guideline is 80 µg m^{-3} (Government of Alberta, 2017). The mean $\pm$ standard deviation of hourly ambient $PM_{2.5}$ concentrations at the AMS sites during the study period in the absence of fire impact ranged from 4.3 ± 4.1 µg m^{-3} at the AMS-21 Conklin community site to 7.1 ± 6.1 µg m^{-3} at the AMS-16 industrial monitoring site. During fire impacted periods, the mean hourly ambient $PM_{2.5}$ concentrations at the AMS sites ranged from 80 ± 67 µg m^{-3} at the AMS-18 regional background site to 293 ± 507 µg m^{-3} at the AMS-7 community monitoring site, representing an average increase of a factor of 18 and 47 at the sites, respectively. The $PM_{2.5}$ concentration enhancements at the WBEA community monitoring sites during fire impact periods ranged from a factor of 19 at AMS-21 (Conklin) to 54 at AMS-6 (Fort McMurray) with associated mean hourly concentrations of 82 ± 62 and 291 ± 673 µg m^{-3}, respectively. WBEA reported 653 hourly $PM_{2.5}$ concentrations in the community sites during the Horse River Fire impact period above the 1-hr $PM_{2.5}$ Alberta Ambient Air Quality Guideline of 80 µg m^{-3}.

Significant enhancements of biomass combustion related pollutants NMHC, NH_3, BC, TRS, NOx, and H_2S were also observed. While NMHC, BC, NOx, and reduced nitrogen compounds such as NH_3 have routinely been measured from wildland fires (Nance et al., 1993; Worden et al., 1997; Dennis et al., 2002), this is the first observation of measurable reduced sulfur compound (TRS/H_2S) emissions. We observed significant correlations between hourly background-corrected NH_3 (ΔNH_3) and background-corrected TRS (ΔTRS) at AMS-6 ($r^2 = 0.948$; Appendix A.9a) and AMS-1 ($r^2 = 0.868$; Appendix A.9b) during smoke impacted periods.

A statistical summary of the fire impacted ambient data from AMS-7 is presented in Table 2, and similar summary tables for the other sites are presented in Appendix B.3a–i. The magnitude of the impact related
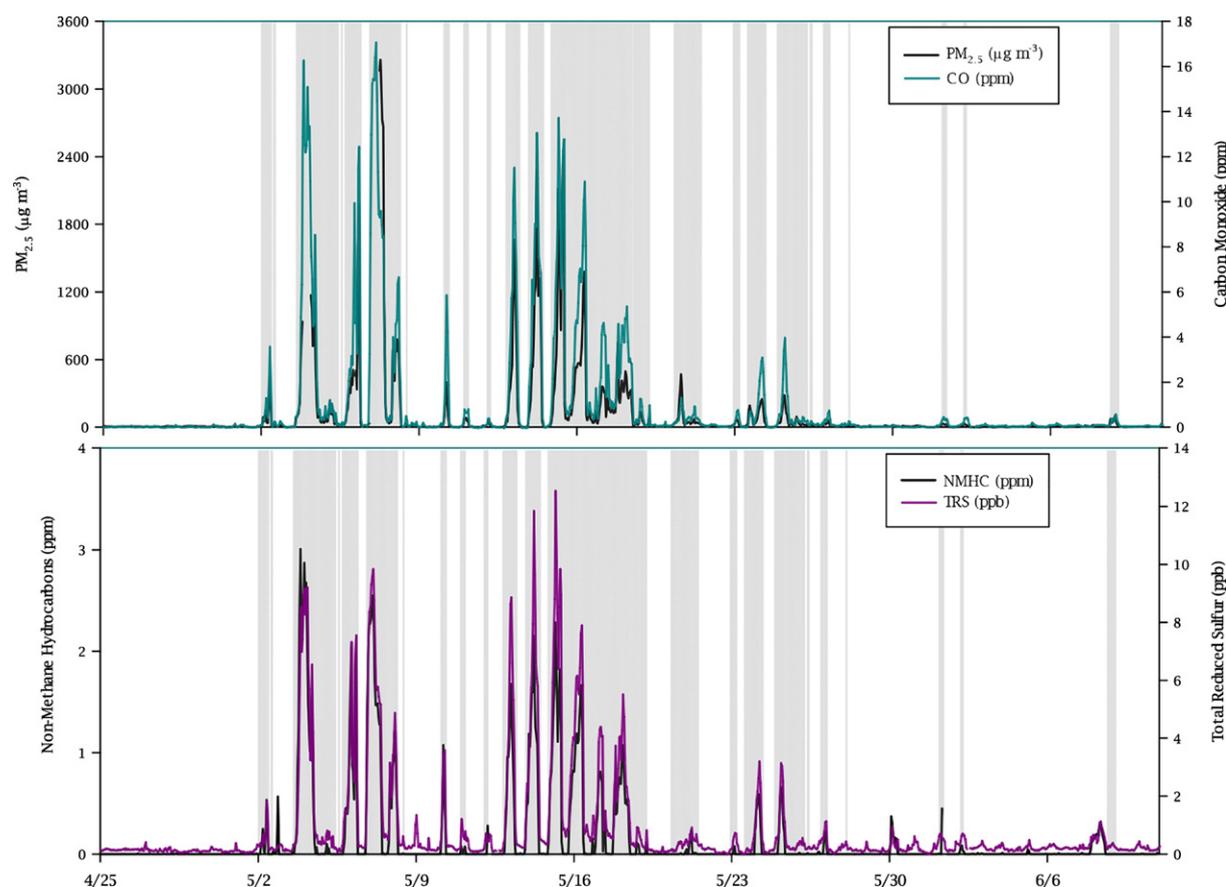
Fig. 2. Times series of AMS-7 Athabasca Valley community monitoring site $PM_{2.5}$, CO, TRS, and NMHC concentrations during the study period (grey highlighting indicates periods categorized as Horse River Fire impacted).

Table 1
Summary of mean ± standard deviation hourly ambient air pollution concentrations (April 1–July 31, 2016) categorized by fire impact.

	AMS-1 No Fire	AMS-1 Fire	AMS-6 No Fire	AMS-6 Fire	AMS-7 No Fire	AMS-7 Fire	AMS-13 No Fire	AMS-13 Fire	AMS-14 No Fire	AMS-14 Fire	AMS-15 No Fire	AMS-15 Fire	AMS-16 No Fire	AMS-16 Fire	AMS-17 No Fire	AMS-17 Fire	AMS-18 No Fire	AMS-18 Fire	AMS-21 No Fire	AMS-21 Fire
Number (n)	2737	191	2515	413	2529	399	2772	156	2476	452	2793	135	2700	228	2746	182	2759	169	2570	164
$PM_{2.5}$ (µg m^{-3})	6.6 ± 6.0	233 ± 585	5.4 ± 5.5	291 ± 673	6.3 ± 5.0	293 ± 507	5.1 ± 4.2	282 ± 711	4.9 ± 4.4	149 ± 403	6.6 ± 6.7	146 ± 307	7.1 ± 6.1	259 ± 826	4.6 ± 4.4	196 ± 219	4.4 ± 3.9	80 ± 67	4.3 ± 4.1	82 ± 62
CH_4 (ppm)	2.0 ± 0.1	2.1 ± 0.2	2.0 ± 0.1	2.2 ± 0.4	1.9 ± 0.1	2.1 ± 0.4			2.0 ± 0.1	2.2 ± 0.9							1.9 ± 0.1	1.9 ± 0.1	1.9 ± 0.1	1.9 ± 0.1
NMHC (ppm)	0.0 ± 0.1	0.2 ± 0.3	0.0 ± 0.0	0.3 ± 0.5	0.0 ± 0.0	0.4 ± 0.7			0.0 ± 0.0	0.2 ± 1.2							0.0 ± 0.0	0.1 ± 0.1	0.0 ± 0.0	0.0 ± 0.0
NO (ppb)	0.7 ± 1.9	0.4 ± 0.8	0.7 ± 1.4	0.8 ± 1.1	1.0 ± 2.4	2.2 ± 4.2	0.7 ± 1.9	0.5 ± 1.1	0.3 ± 1.5	2.3 ± 15.9	1.0 ± 3.8	0.5 ± 1.5	4.9 ± 9.7	3.8 ± 9.9	0.4 ± 0.6	0.1 ± 0.6	0.1 ± 0.1	0.1 ± 0.2	0.2 ± 0.9	0.1 ± 0.2
NO_2 (ppb)	3.4 ± 4.2	5.4 ± 7.0	2.7 ± 2.9	5.8 ± 7.9	3.5 ± 2.9	7.7 ± 8.3	3.0 ± 3.8	4.9 ± 6.5	1.1 ± 1.1	4.7 ± 19.2	3.1 ± 4.1	6.1 ± 7.6	6.2 ± 6.5	7.0 ± 8.1	1.1 ± 1.7	5.1 ± 4.6	0.8 ± 0.5	2.7 ± 1.6	1.0 ± 0.9	2.3 ± 1.4
NO_X (ppb)	4.0 ± 5.4	5.7 ± 7.6	3.4 ± 3.8	6.5 ± 8.3	4.4 ± 4.1	9.8 ± 10.6	3.7 ± 5.1	5.3 ± 7.4	1.5 ± 2.1	6.5 ± 35.1	4.1 ± 7.0	6.6 ± 8.6	11.2 ± 15.2	10.9 ± 15.5	1.3 ± 2.0	4.4 ± 4.5	0.8 ± 0.6	2.8 ± 1.6	1.2 ± 1.5	2.4 ± 1.5
O_3 (ppb)	27 ± 13	34 ± 16	33 ± 11	39 ± 26	28 ± 11	41 ± 41	25 ± 14	31 ± 16	31 ± 12	38 ± 101					31 ± 12	39 ± 12	38 ± 10	43 ± 11	31 ± 14	32 ± 15
SO_2 (ppb)	0.9 ± 3.6	1.8 ± 4.2	1.0 ± 3.0	1.0 ± 1.7	0.9 ± 2.1	1.7 ± 4.0	0.9 ± 3.6	1.7 ± 4.2	0.5 ± 0.5	1.8 ± 5.2	0.5 ± 1.9	1.1 ± 1.3	0.8 ± 2.4	1.5 ± 3.3	0.5 ± 1.3	1.4 ± 1.6	0.3 ± 0.3	1.8 ± 1.6	0.3 ± 0.3	0.3 ± 0.2
THC (ppm)	2.0 ± 0.2	2.3 ± 0.6	2.0 ± 0.1	2.4 ± 0.9	1.9 ± 0.1	2.6 ± 1.1	2.3 ± 0.4	2.8 ± 1.2	2.0 ± 0.1	2.4 ± 2.1	2.2 ± 0.3	2.4 ± 0.5	2.4 ± 0.4	2.7 ± 0.5	2.1 ± 0.1	2.5 ± 0.4	2.0 ± 0.1	2.0 ± 0.1	1.9 ± 0.1	1.9 ± 0.1
TRS (ppb)	0.5 ± 0.2	1.2 ± 1.3	0.2 ± 0.1	1.3 ± 2.4	0.3 ± 0.2	2.2 ± 2.6	0.2 ± 0.3	0.9 ± 1.5	0.2 ± 0.1	1.4 ± 3.3	0.3 ± 0.7	0.7 ± 1.0					0.3 ± 0.0	0.5 ± 0.2	0.4 ± 0.2	0.4 ± 0.2
BC (µg m^{-3})	0.3 ± 0.4	3.3 ± 6.4															0.1 ± 0.2	2.5 ± 2.2		
Delta-C (µg m^{-3})	0.1 ± 0.2	20 ± 162															0.1 ± 0.3	8.0 ± 8.2		
NH_3 (ppb)	1.4 ± 1.2	25 ± 39	3.3 ± 4.1	136 ± 221																
CO (ppm)					0.1 ± 0.0	2.8 ± 3.7														
H_2S (ppb)															0.1 ± 0.1	0.5 ± 0.5				

Table 2
Statistical summary of AMS-7 site hourly ambient air pollution concentrations (April 1–July 31, 2016) during Horse River Fire impact periods.

Species	Unit	Mean	25th percentile	Median	75th percentile	Maximum
CO	ppm	2.8	0.4	0.8	4.0	17.1
$PM_{2.5}$	µg m^{-3}	293	33	91	308	3259
THC	ppm	2.6	1.9	2.0	3.0	6.6
CH_4	ppm	2.1	1.9	1.9	2.3	3.7
NMHC	ppm	0.4	0.0	0.0	0.7	3.0
NO	ppb	2.2	0.3	1.0	2.2	35.2
NO_2	ppb	7.7	2.5	4.9	10.0	54.3
NO_X	ppb	9.8	3.1	5.7	12.5	61.0
TRS	ppb	2.2	0.5	0.8	3.3	12.6
SO_2	ppb	1.7	0.2	0.7	1.4	36.1
O_3	ppb	41	20	30	45	358

to the Horse River Fire emissions are highlighted at many of the AMS sites where the mean observed concentrations of fire related pollutants (e.g., $PM_{2.5}$, TRS, NH_3, NO, NO_2, NO_X, CH_4, NMHC, SO_2) exceed their 75th percentile value concentrations. The maximum hourly fire impacted $PM_{2.5}$ concentrations at the community sites ranged from 357 µg m^{-3} (AMS-21) to 5229 µg m^{-3} (AMS-6), representing extremely high and unhealthy acute exposures to firefighting personnel working in these communities and citizens not heeding evacuation orders. The ambient $PM_{2.5}$ concentrations measured at the AMS community sites during fire impact periods are on the same order as $PM_{2.5}$ concentrations that have been reported for wildland firefighter occupational exposures (Naeher et al., 2006; Miranda et al., 2010; Adetona et al., 2011), and in some cases higher by >2 orders of magnitude above downwind community monitoring sites where observable public health effects were documented (Lee et al., 2014; Liu et al., 2015; Reid et al., 2016; Adetona et al., 2016; Kim et al., 2017). Ambient $PM_{2.5}$ measurements made as part of past routine community monitoring programs and emergency response operations in many cases have not reported concentrations above 800–1000 µg m^{-3} due to inherent limitations of the continuous monitoring instruments (Bytnerowicz et al., 2016; Schweizer et al., 2016) and filter loading related flow restrictions on integrated samplers (Landis et al., 2017). Unfortunately, carbon dioxide (CO_2) measurements were not part of the WBEA AMS routine monitoring plan in 2016, so modified combustion efficiencies (Urbanski, 2013) could not be calculated; and the measured ambient concentrations could not be categorized in terms of fire combustion regime (e.g., flaming, smoldering).

The reported elevated "O_3" concentrations reached a maximum hourly concentration of 1586 ppb at AMS-14, and appeared to be a smoke (volatile organic compound) induced measurement artifact from the WBEA UV photometric instruments, as have been previously reported (Kleindienst et al., 1993; United States Environmental Protection Agency, 1999a, 1999b; Spicer et al., 2010). Elevated "O_3" concentrations were observed at night (22:00–05:00) in the absence of photochemistry and were positively correlated with NO and NMHC. The significant relationships between nighttime "O_3", NO, and NMHC at sites AMS-14 (May 5) and AMS-6 (May 4) are presented in Appendices A.10a–b, respectively. Nighttime 5-min "O_3" concentrations reached 7077 ppb at AMS-14 and 361 ppb at AMS-6. These observations raise concerns that regulatory O_3 measurements utilizing UV photometric Federal Equivalent Method (FEM) instruments may be reporting false positive results, and that the reported hypothesis that rapid photochemical processing was responsible for observed elevated O_3 concentrations reported in downwind wildfire plumes may be influenced analytical artifacts (e.g., Liu et al., 2017). EPA is currently evaluating

Federal Reference Method (FRM) and photometric FEM instruments for positive O_3 artifact response in wildland fire smoke.

3.2. Emission ratios

Emissions of air pollutants from wildfires are commonly expressed as normalized emission ratios (ER) where the excess in each analyte X in a smoke plume above its background value ($\Delta X = X_{plume} - X_{background}$) is divided by a simultaneously measured excess mixing ratio ($\Delta Y = Y_{plume} - Y_{background}$) of a relatively inert tracer gas like CO (Yokelson et al., 1999; Yokelson et al., 2009; Akagi et al., 2011; Hecobian et al., 2011; Hornbrook et al., 2011; Simpson et al., 2011; O'Shea et al., 2013; Urbanski, 2013; Collier et al., 2016; Liu et al., 2017). In this case, the $ER_{X/CO}$ were calculated for all air pollutants measured at the AMS-7 monitoring site through the linear regression of hourly averaged background corrected ambient concentrations where the regression intercept was forced through zero (Yokelson et al., 1999). The background normalization for each hourly integrated data point categorized as smoke impacted was calculated by subtracting the median site concentration during periods categorized as non-smoke impacted during the fire event period (Table 3). The AMS-7 background for CO was 93 ± 2 ppb (median ± variance) which compared quite well to the values of 105 ± 9 ppb reported by O'Shea et al. (2013) for Eastern Canada and 97 ± 6 ppb reported by Cofer et al. (1998) for the Canadian Northwest Territories.

The $ER_{\Delta X/\Delta CO}$ regressions are presented in Fig. 3a–i and summarized in Table 3 for $PM_{2.5}$ (149.87 ± 3.37 μgm^{-3} ppm^{-1}; slope ± standard error), THC (0.274 ± 0.002 ppm ppm^{-1}), NMHC (0.169 ± 0.001 ppm ppm^{-1}), CH_4 (0.104 ± 0.001 ppm ppm^{-1}), TRS (0.694 ± 0.007 ppb ppm^{-1}), SO_2 (0.519 ± 0.040 ppb ppm^{-1}), NO (0.412 ± 0.045 ppb ppm^{-1}), NO_2 (1.968 ± 0.053 ppb ppm^{-1}), and NO_X (2.337 ± 0.077 ppb ppm^{-1}). While the $ER_{\Delta PM2.5/\Delta CO}$ could include secondary $PM_{2.5}$ formed after emission, given the proximity of the wildfire it was likely that primary $PM_{2.5}$ was dominant. The ER regressions for THC, NMHC, CH_4, and TRS were extremely well fit over a wide range of smoke impacts representing ~400 h of measurements resulting in relatively low standard errors. The ER regressions for $PM_{2.5}$, SO_2, NO, NO_2, and NO_X demonstrated more variance that may be related to changing burn conditions (e.g., flaming, smoldering) during the fire impact periods (Urbanski, 2013) resulting in larger standard errors. The five AMS-7 $PM_{2.5}$ observations that were >2500 μg m^{-3} and fall outside the regression 95% confidence internal (Fig. 3a) were all observed on May 7, 2016 from 06:00–10:00, however no other associated observations during this time period were similarly documented as regression outliers.

The ERs observed during the Horse River Fire generally compared well to other boreal forest fire results reported in the literature as

summarized in Table 4. The Horse River Fire ERs for CH_4 (0.104 ± 0.001 ppm ppm^{-1}), SO_2 (0.519 ± 0.040 ppb ppm^{-1}), and NO_X (2.337 ± 0.077 ppb pm^{-1}) agree within reported uncertainties with "fresh biomass burning" plumes ($n = 18$) measured from aircraft at altitudes 2.0 ± 1.3 km reported by Singh et al. (2010). The Horse River Fire ER for CH_4 agrees within reported uncertainties, the ER for NO_2 (1.968 ± 0.053 ppb ppm^{-1}) is approximately a factor of three lower, and the ER for NO (0.412 ± 0.045 ppb ppm^{-1}) is approximately a factor of six lower than whole air sampling of Canadian boreal forest fire plumes ($n = 7$) measured from ground and aircraft platforms as reported by Simpson et al. (2011). The Horse River Fire ER for NO_X agrees within reported uncertainties, and the ER for CH_4 is approximately a factor of four lower than whole air samples of forest fire plumes measured from seventeen aircraft flights reported by Hecobian et al. (2011) from Canadian boreal and California fires. The Horse River Fire ERs for CH_4 is approximately 30% higher than the 0.079 ± 0.001 ppm ppm^{-1} reported by O'Shea et al. (2013) measured from fifteen aircraft flights of eastern Canadian forest fires.

3.3. Impact of fire emissions on forest health site monthly integrated concentrations

HNO_3 and NH_3 concentrations for calendar year 2016 (CY2016) are presented in Fig. 4a–b. Data are segregated into three time periods corresponding to non-fire impacted samples ($n = 10$–11 per site), fire impacted samples (1 per site), and the annual average. Due to variable sample durations, non-fire impacted and annual concentrations are calculated as time-weighted averages. For HNO_3 (Fig. 4a) CY2016 concentrations are highest at JP104 and JP107 followed by JP213 and then JP201, and there is virtually no difference between fire impacted samples and non-fire impacted samples. Inspection of $PM_{2.5}$ nitrate data from site JP104 shows that concentrations during the fire period were roughly 4 times higher than the non-fire period, and roughly 3 times higher than HNO_3 during the fire period. This suggests that the majority of HNO_3 produced during, or subsequent to, the fire partitioned into the particulate phase, due to reaction with abundant NH_3 or relatively alkaline pyrogenic PM. For NH_3, the order of CY2016 concentrations is somewhat different, with JP104 > JP213 > JP107 > JP201. More importantly, there are striking NH_3 concentration differences between fire and non-fire impacted samples at all sites (Fig. 4b). For JP104 and JP213, NH_3 concentrations in fire samples are roughly 14 times higher than non-fire samples. At JP107 and JP201, fire samples are roughly 7 and 2 times higher than non-fire samples. Expressed another way, the sample collected during the Horse River Fire event contributed about 65% of the annual time-weighted average NH_3 at JP104 and JP107, 80% at JP213, and 25% at JP201.

These observations show that short-term emissions from wildland fires can have a marked impact on annual concentrations of NH_3 as well as a potentially significant impact on nutrient loadings to terrestrial and aquatic ecosystems in the AOSR. This finding is consistent with Benedict et al. (2017) who observed hourly NH_3 enhanced by a factor of ~20 in wildfire smoke-impacted periods in Fort Collins, Colorado. However, the same study found a more moderate wildfire enhancement (~2–3 times) for daily integrated denuder NH_3 as well as HNO_3 measurements. The difference in magnitude between the NH_3 enhancement observed in the AOSR as a result of the Horse River Fire and the results reported by Benedict et al. (2017) are likely the result of differences in NH_3 emission as observed by the $\Delta NH_3/\Delta NO_X$ at AMS-6 (21.0; Appendix A.11a), AMS-1 (3.6; Appendix A.11b), and ~2.5–3.0 reported by Benedict et al. (2017) (Fig. 4b). It is possible the Benedict et al. (2017) observed increase in HNO_3 was due to the larger distance from the flame front, allowing time for the oxidation of NO_X into HNO_3, or less partitioning to the particulate phase than was observed in this study.

The $PM_{2.5}$ mass and trace element results (JP104 only) show two interesting patterns that include the majority of measured analytes (Fig.

Table 3

Statistical summary of AMS-7 normalized excess mixing ratios (NEMRs) of air pollutants during Horse River Fire impacted hourly time periods calculated using normal linear regression (all $p < 0.0001$).

Compound	Background[a]	NEMR[b]	r^2
CO	0.093 ± 0.002 ppm	n/a	n/a
$PM_{2.5}$	5.08 ± 14.88 μg m^{-3}	149.87 ± 3.37 μg m^{-3} ppm^{-1}	0.8402
THC	1.855 ± 0.007 ppm	0.274 ± 0.002 ppm ppm^{-1}	0.9782
NMHC	0.000 ± 0.002 ppm	0.169 ± 0.001 ppm ppm^{-1}	0.9777
CH_4	1.855 ± 0.003 ppm	0.104 ± 0.001 ppm ppm^{-1}	0.9587
TRS	0.239 ± 0.020 ppb	0.694 ± 0.007 ppb ppm^{-1}	0.9590
SO_2	0.167 ± 1.761 ppb	0.519 ± 0.040 ppb ppm^{-1}	0.3062
NO	0.641 ± 14.356 ppb	0.412 ± 0.045 ppb ppm^{-1}	0.1774
NO_2	1.750 ± 7.514 ppb	1.968 ± 0.053 ppb ppm^{-1}	0.7764
NO_X	2.530 ± 25.965 ppb	2.337 ± 0.077 ppb ppm^{-1}	0.7012

[a] Background = Median ± variance of non-fire impacted ambient hourly sample concentrations during fire period (number of observations ranged from 723 to 726). Median value used to normalize each hourly observation to calculate ΔX.

[b] NEMR = slope of linear regression ΔX and ΔCO when intercept forced through zero ± standard error.

Fig. 3. Scatter plots of background-corrected analytes versus ΔCO for (a) $\Delta PM_{2.5}$, (b) ΔTHC, (c) $\Delta NMHC$, (d) ΔCH_4, (e) ΔTRS, (f) ΔSO_2, (g) ΔNO, (h) ΔNO_2, and (i) ΔNO_X for Hourly AMS-7 Horse River Fire impacted samples.

3c). For refractory elements (e.g., Si, Mo, Ni, V, Ce, Th, U), we observed significantly lower concentrations during the Horse River Fire event than the rest of the year. This likely reflects the temporary shutdown of oil sands mining and bitumen upgrading operations during and immediately after the fire, with mining having been previously shown to be a dominant source of fugitive dust in the region (Landis et al.,

Table 4
Comparison of this study's NEMRs to other literature values for North American boreal forest wildfires.

Compound	Unit	This study	O'Shea et al. (2013)	Hecobian et al. (2011)	Simpson et al. (2011)	Singh et al. (2010)
PM$_{2.5}$	µg m^{-3} ppm^{-1}	149.87 ± 3.37				
THC	ppm ppm^{-1}	0.274 ± 0.002				
NMHC	ppm ppm^{-1}	0.169 ± 0.001				
CH$_4$	ppm ppm^{-1}	0.104 ± 0.001	0.079 ± 0.001	0.478 ± 0.199	0.072 ± 0.044	0.08 ± 0.03
TRS	ppb ppm^{-1}	0.694 ± 0.007				
SO$_2$	ppb ppm^{-1}	0.519 ± 0.040				1.1 ± 0.6
NO	ppb ppm^{-1}	0.412 ± 0.045			2.4 ± 0.1	
NO$_2$	ppb ppm^{-1}	1.968 ± 0.053			5.6 ± 0.3	
NO$_X$	ppb ppm^{-1}	2.337 ± 0.077		1.721 ± 2.196		3.5 ± 4.2
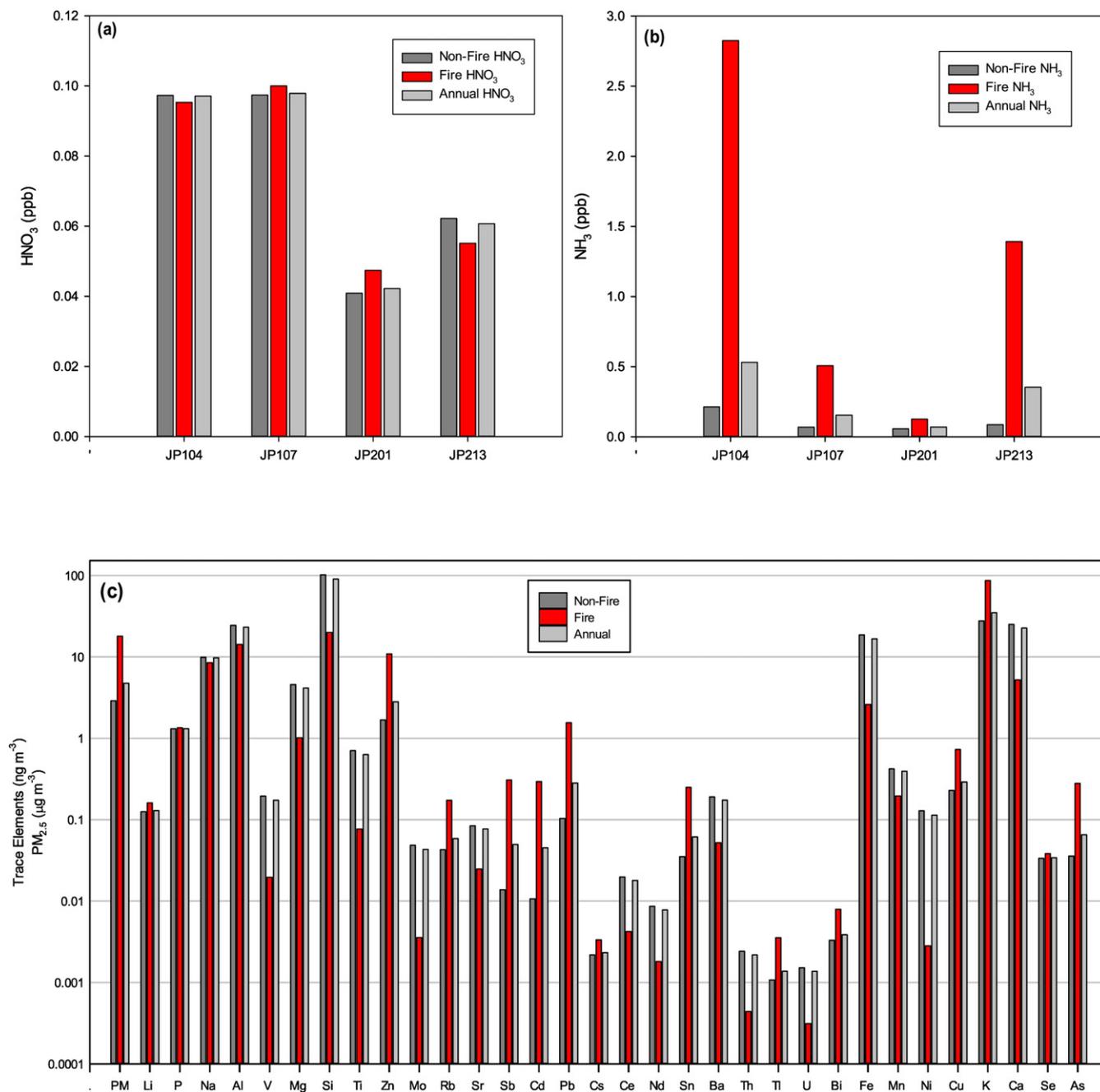
Fig. 4. Forest health monitoring monthly sampling results for (a) HNO_3, (b) NH_3, and (c) $PM_{2.5}$ and trace elements quantifying the Horse River Fire impact.

2012; Landis et al., 2017). In addition, upgrader emissions and "mixed sources" have been identified as major contributors to Mo, V, and Ni at AMS-5, AMS-11, and AMS-13, whereas K and Cd were found to be tracers for biomass burning (Phillips-Smith et al., 2017), consistent with Fig. 4c. The second group includes volatile elements and oxides that are markedly enhanced during the fire. These include Rb, Tl, and K (3–4 times higher), Zn, As and Sn (6–10 times higher) and Sb, Cd, Pb (15–27 times higher). The wildland fire impact on Sb, Cd and Pb more than doubled their respective annual time-weighted concentrations, which suggests that inter-annual variability of these elements (like NH_3) may be driven by local and regional wildland fires.

3.4. AMS site filter-based $PM_{2.5}$ mass reconstruction

Table 4 summarizes the $PM_{2.5}$ mass reconstruction from each of the AMS sample filters that were analyzed for carbohydrates, OC, and EC

(including both fire impacted and non-fire impacted days). Carbon was integrated into the $PM_{2.5}$ composition analysis by using the TOR OC and EC values from the AMS-1 quartz filter samples, and the FTIR OC and EC measurements from the AMS-6/AMS-7 Teflon filter samples. OC results were multiplied by 1.76 to obtain total organic matter (OM) which accounts for associated oxygen and hydrogen mass (Aiken et al., 2008). OM was the major constituent on both fire impacted and non-impacted sample days. On August 4, 2016, a sampling day with no fire impact, $PM_{2.5}$ concentrations at the AMS-1, AMS-6, and AMS-7 community sites was 8.0 ± 0.8 μg m^{-3} (mean ± standard deviation) and OM represented ~60% of the total mass with ~1.5% from the sum of all carbohydrates (ΣSugar; Appendix A.12a). On fire impacted days at sites AMS-6 and AMS-7, the mean $PM_{2.5}$ concentration was 125 μg m^{-3} and OM represented ~90% of mass with ~25% from ΣSugar (Table 5). Levoglucosan is an anhydrosugar produced from the combustion of cellulose and a well-established tracer for biomass combustion (Sullivan

Table 5
Reconstructed $PM_{2.5}$ mass for filter samples with enhanced analytical results.

Component ($\mu g\ m^{-3}$)	AMS-1			AMS-6		AMS-7	
	Fire impacted		No fire	Fire impacted	No fire	Fire impacted	No fire
	May 18	May 24	August 4	May 18	August 4	May 12	August 4
$PM_{2.5}$ Mass	25.8	42.2	7.1	139.0	8.4	110.5	8.4
ΣSugar OC	1.0 (3.8%)	5.6 (13.3%)	0.1 (1.9%)	38.5 (27.7%)	0.1 (1.3%)	25.5 (23.0%)	0.1 (1.3%)
Other organic matter[a]	13.6 (52.7%)	26.2 (62.1%)	4.7 (66.0%)	84.6 (60.9%)	4.1 (49.0%)	69.6 (63.0%)	4.8 (57.4%)
Crustal[b]	8.34 (32.3%)	6.31 (14.9%)	1.98 (27.9%)	0.85 (0.6%)	1.61 (19.2%)	0.93 (0.8%)	1.52 (18.1%)
Elemental carbon	0.50 (2.0%)	1.66 (4.0%)	0.32 (4.5%)	16.6 (11.9%)	0.30 (3.6%)	15.7 (14.2%)	0.40 (4.8%)
Sulfate	0.38 (1.5%)	0.87 (2.1%)	0.38 (5.4%)	0.62 (0.4%)	0.86 (10.3%)	0.84 (0.8%)	1.08 (12.8%)
Nitrate	0.16 (0.6%)	0.30 (0.7%)	0.07 (1.0%)	0.20 (0.1%)	0.14 (1.8%)	0.06 (0.0%)	0.10 (1.3%)
Ammonium	0.13 (0.5%)	0.19 (0.5%)	0.11 (1.6%)	0.50 (0.4%)	0.24 (2.9%)	0.39 (0.4%)	0.31 (3.7%)
TEO[c]	0.66 (2.6%)	0.76 (1.8%)	0.10 (1.5%)	0.82 (0.6%)	0.10 (1.3%)	0.28 (0.3%)	0.11 (1.4%)
Unexplained mass	1.01 (3.9%)	0.22 (0.5%)	0.70 (9.8%)	−4.02 (−2.9%)	0.89 (10.6%)	−2.94 (−2.7%)	−0.07 (−0.8%)

[a] Other Organic Matter = (OC * 1.76) - ΣSugar OC.
[b] Chow et al. (2015).
[c] Landis et al. (2001).

et al., 2011a; Sullivan et al., 2011b; Sullivan et al., 2014). During the Horse River Fire levoglucosan was strongly correlated with pooled PM_{10} and $PM_{2.5}$ mass ($r^2 = 0.954$; Appendix A.13a), and other anhydrosugars mannosan ($r^2 = 0.993$; Appendix A.13b) and galactosan ($r^2 = 0.980$; Appendix A.13c) across the WBEA network.

Two additional summary variables were calculated including a soil or crustal variable calculated as the sum of oxides of crustal elements (Chow et al., 2015), and trace element oxides (TEO) which was calculated as the sum of other atmospheric metal oxides (Landis et al., 2001). On average, the PM mass collected in the AOSR were well attributed with <5% absolute mass left unexplained. Horse River Fire source profiles were developed from each of the fire impacted samples in Table 5 by dividing the chemical concentration for each sample by the total mass on the filter. The resulting profiles (Appendix A.14) were fairly uniform across the network, are in good agreement with the profiles previously observed during the 2011 Richardson Backcountry Fire reported by Landis et al. (2012), and can be used as a "fingerprint" for fire influence in future studies in northern Alberta.

4. Conclusions

Smoke from the 2016 Horse River Fire had a major air quality impact on the city of Fort McMurray and other communities in the AOSR resulting in 188 exceedances of 1-hr and 24-hr AAAQOs, and Air Quality Health Index (AQHI) "very high" health risk designations. The ambient $PM_{2.5}$ concentrations measured at the AMS community sites during fire impact periods are on the same order as $PM_{2.5}$ concentrations that have been reported for wildland firefighter occupational exposures, and in some cases higher by >2 orders of magnitude above ambient community concentrations where public health effects from wildland fire smoke were documented. The $PM_{2.5}$ concentration enhancements at the six WBEA community monitoring sites during fire impact periods ranged from a factor of 19 at the AMS-21 (Conklin) site to 54 at the AMS-6 (Fort McMurray) site with associated mean/maximum hourly concentrations of 82/357 $\mu g\ m^{-3}$ and 291/5229 $\mu g\ m^{-3}$, respectively. The highest maximum hourly $PM_{2.5}$ concentration of 6106 $\mu g\ m^{-3}$ was observed at the AMS-16 Muskeg River Industrial site (Appendix B.3f).

Significant enhancements of biomass combustion related pollutants NMHC, NH_3, BC, Delta-C, TRS, NOx, and H_2S were also observed across the WBEA network; this is the first observation of measurable reduced sulfur compound (TRS/H_2S) emissions from a wildfire. Normalized excess emission ratios were calculated from ~400 hourly Horse River Fire impacted observations at the AMS-7 for $PM_{2.5}$ (149.87 ± 3.37 $\mu g\ m^{-3}\ ppm^{-1}$), THC (0.274 ± 0.002 ppm ppm^{-1}), NMHC (0.169 ± 0.001 ppm ppm^{-1}), CH_4 (0.104 ± 0.001 ppm ppm^{-1}), TRS (0.694 ± 0.007 ppb ppm^{-1}), SO_2 (0.519 ± 0.040 ppb ppm^{-1}), NO (0.412 ±

0.045 ppb ppm^{-1}), NO_2 (1.968 ± 0.053 ppb ppm^{-1}), and NO_X (2.337 ± 0.077 ppb ppm^{-1}). The emission of NH_3 from the Horse River Fire also had a pronounced impact on annual concentrations measured at the WBEA forest health monitoring sites (up to ~14 times higher than non-fire impacted periods), as well as the resulting potential nutrient loadings to terrestrial and aquatic ecosystems in the AOSR. Filter-based $PM_{2.5}$ samples impacted by Horse River Fire emissions exhibited enhancements in smoke related constituents such as OM, representing ~90% of mass with ~25% of that mass from ΣSugar (primarily levoglucosan, mannosan, and galactosan). The Horse River Fire source profiles were fairly uniform across the network, and can be used as a "fingerprint" for fire influence in future studies in northern Alberta.

Appendix A. Supplementary data

Supplementary data to this article can be found online at https://doi.org/10.1016/j.scitotenv.2017.10.008.

References

Adetona, O., Dunn, K., Hall, D.B., Achtemeier, G., Stock, A., Naeher, L.P., 2011. Personal $PM_{2.5}$ exposure among wildland firefighters working at prescribed forest burns in Southeastern United States. J. Occup. Environ. Hyg. 8 (8):503–511. https://doi.org/10.1080/15459624.2011.595257.

Adetona, O., Reinhardt, T.E., Domitrovich, J., Broyles, G., Adetona, A.M., Kleinman, M.T., Ottmar, R.D., Naeher, L.P., 2016. Review of the health effects of wildland fire smoke on wildland fire fighters and the public. Inhal. Toxicol. 28 (3):95–139. https://doi.org/10.3109/08958378.2016.1145771.

Aiken, A.C., DeCarlo, P.F., Kroll, J.H., Worsnop, D.R., Huffman, J.A., Docherty, K.S., Ulbrich, I.M., Mohr, C., Kimmel, J.R., Sueper, D., Sun, Y., Zhang, Q., Trimborn, A., Northway, M., Ziemann, P.J., Canagaratna, M.R., Onasch, T.B., Alfarra, M.R., Prevot, A.S.H., Dommen, J., Duplissy, J., Metzger, A., Baltensperger, U., Jimenez, J.L., 2008. O/C and

OM/OC ratios of primary, secondary, and ambient organic aerosols with high resolution time-of-flight aerosol mass spectrometry. Environ. Sci. Technol. 42:4478–4485. https://doi.org/10.1021/es703009q.

Akagi, S.K., Yokelson, R.J., Wiedinmyer, C., Alvarado, M.J., Reid, J.S., Karl, T., Crounse, J.D., Wennberg, P.O., 2011. Emission factors for open and domestic biomass burning for use in atmospheric models. Atmos. Chem. Phys. 11:4039–4072. https://doi.org/10.5194/acp-11-4039-2011.

Alberta Agriculture and Forestry, 2017. Historical Wildfire Database. Last Accessed September 19. http://wildfire.alberta.ca/resources/historical-data/historical-wildfire-database.aspx.

Allen, G.A., Babich, P., Poirot, R.L., 2004. Evaluation of a new approach for real-time assessment of wood smoke PM. Proceedings of the Regional and Global Perspectives on Haze: Causes, Consequences, and Controversies, Air and Waste Management Association Visibility Specialty Conference, Asheville, NC paper #16.

Baker, K.R., Woody, M.C., Tonnesen, G.S., Hutzell, W., Pye, H.O.T., Beaver, M.R., Pouliot, G., Pierce, T., 2016. Contribution of regional-scale fire events to ozone and PM2.5 air quality estimated by photochemical modeling approaches. Atmos. Environ. 140: 539–554. https://doi.org/10.1016/j.atmosenv.2016.06.032.

Benedict, K.B., Prenni, A.J., Carrico, C.M., Sullivan, A.P., Schichtel, B.A., Collett Jr., J.L., 2017. Enhanced concentrations of reactive nitrogen species in wildfire smoke. Atmos. Environ. 148:8–15. https://doi.org/10.1016/j.atmosenv.2016.10.030.

Bytnerowicz, A., Hsu, Y.M., Percy, K., Legge, A., Fenn, M.E., Schilling, S., Fraczek, W., Alexander, D., 2016. Ground-level air pollution changes during a boreal wildland mega-fire. Sci. Total Environ. 572:755–769. https://doi.org/10.1016/j.scitotenv.2016.07.052.

Canadian Forest Service, 2016. National Fire Database – Agency Fire Data. Natural Resources Canada, Northern Forestry Centre, Edmonton, Alberta.

Chow, J.C., Watson, J.G., Pritchett, L.C., Pierson, W.R., Frazier, C.A., Purcell, R.G., 1993. The DRI Thermal/Optical Reflectance carbon analysis system: description, evaluation and applications in U.S. air quality studies. Atmos. Environ. 27A (8):1185–1201. https://doi.org/10.1016/0960-1686(93)90245-T.

Chow, J.C., Watson, J.G., Chen, L.W.A., Chang, M.C.O., Robinson, N.F., Trimble, D., Kohl, S., 2007. The IMPROVE-A temperature protocol for thermal/optical carbon analysis: maintaining consistency with a long-term database. J. Air Waste Manage. Assoc. 57: 1014–1023. https://doi.org/10.3155/1047-3289.57.9.1014.

Chow, J.C., Lowenthal, D.H., Chen, L.W.A., Wang, X., Watson, J.G., 2015. Mass reconstruction methods for PM2.5: a review. Air Qual. Atmos. Health 8:243–263. https://doi.org/10.1007/s11869-015-0338-3.

Cofer III, W.R., Winstead, E.L., Stocks, B.J., Goldammer, J.G., Cahoon, D.R., 1998. Crown fire emissions of CO2, CO, H2, CH4, and TNMHC from a dense jack pine boreal forest fire. Geophys. Res. Lett. 25:3919–3922. https://doi.org/10.1029/1998GL900042.

Collier, S., Zhou, S., Onasch, T.B., Jaffe, D.A., Kleinman, L., Sedlacek III, A.J., Briggs, N.L., Hee, J., Fortner, E., Shilling, J.E., Worsnop, D., Yokelson, R.J., Parworth, C., Ge, H., Xu, J., Butterfield, Z., Chand, D., Dubey, M.K., Pekour, M.S., Springston, S., Zhang, Q., 2016. Regional influence of aerosol emissions from wildfires driven by combustion efficiency: insights from the BBOP campaign. Environ. Sci. Technol. 50:8613–8622. https://doi.org/10.1021/acs.est.6b01617.

Dennis, A., Fraser, M., Anderson, S., Allen, D., 2002. Air pollutant emissions associated with forest, grassland, and agricultural burning in Texas. Atmos. Environ. 36:3779–3792. https://doi.org/10.1016/S1352-2310(02)00219-4.

Donahue, N.M., Robinson, A.L., Pandis, S.N., 2009. Atmospheric organic particulate matter: from smoke to secondary organic aerosol. Atmos. Environ. 43:94–106. https://doi.org/10.1016/j.atmosenv.2008.09.055.

Drinovec, L., Močnik, G., Zotter, P., Prévôt, A.S.H., Ruckstuhl, C., Coz, E., Rupakheti, M., Sciare, J., Müller, T., Wiedensohler, A., Hansen, A.D.A., 2015. The "dual-spot" Aethalometer: an improved measurement of aerosol black carbon with real-time loading compensation. Atmos. Meas. Tech. 8:1965–1979. https://doi.org/10.5194/amt-8-1965-2015.

Edgerton, E.S., Fort, J.M., Baumann, K., Graney, J.R., Landis, M.S., Berryman, S., Krupa, S., 2012. Method for extraction and multi-element analysis of *Hypogymnia Physodes* samples from the Athabasca Oil Sands Region. In: Percy, Kevin (Ed.), Alberta Oil Sands: Energy, Industry and the Environment. Elsevier, Oxford, England.

Government of Alberta, 2017. Alberta Ambient Air Quality Objectives and Guidelines Summary, AEP, Air Policy, 2016, No. 2, June 29, 2017. Last accessed September 19. http://aep.alberta.ca/air/legislation/ambient-air-quality-objectives/documents/AAQO-Summary-Jun29-2017.pdf.

Hecobian, A., Liu, Z., Hennigan, C.J., Huey, L.G., Jimenez, J.L., Cubison, M.J., Vay, S., Diskin, G.S., Sachse, G.W., Wisthaler, A., Mikoviny, T., Weinheimer, A.J., Liao, J., Knapp, D.J., Wennberg, P.O., Kürten, A., Crounse, J.D., St. Clair, J., Wang, Y., Weber, R.J., 2011. Comparison of chemical characteristics of 495 biomass burning plumes intercepted by the NASA DC-8 aircraft during the ARCTAS/CARB-2008 field campaign. Atmos. Chem. Phys. 11:13325–13337. https://doi.org/10.5194/acp-11-13325-2011.

Hornbrook, R.S., Blake, D.R., Diskin, G.S., Fried, A., Fuelberg, H.E., Meinardi, S., Mikoviny, T., Richter, D., Sachse, G.W., Vay, S.A., Walega, J., Weibring, P., Weinheimer, A.J., Wiedinmyer, C., Wisthaler, A., Hills, A., Riemer, D.D., Apel, E.C., 2011. Observations of nonmethane organic compounds during ARCTAS – part 1: biomass burning emissions and plume enhancements. Atmos. Chem. Phys. 11:11103–11130. https://doi.org/10.5194/acp-11-11103-2011.

Kim, Y.H., Warren, S., Krantz, Q.T., King, C., Jaskot, R., Preston, W.T., George, B.J., Hays, M.D., Landis, M.S., Higuchi, M., DeMarini, D., Gilmour, M.I., 2017. Mutagenicity and lung toxicity of smoldering versus flaming emissions from various biomass fuels: implications for health effects from wildland fires. Environ. Health Perspect. (In Press).

Kitzberger, T., Brown, P.M., Heyerdahl, E.K., Swetnam, T.W., Veblen, T.T., 2007. Contingent Pacific–Atlantic Ocean influence on multi-century wildfire synchrony over western North America. P. Natl. Acad. Sci. USA 104 (2):543–548. https://doi.org/10.1073/pnas.0606078104.

Kleindienst, T.E., Hudgens, E.R., Smith, D.F., McElroy, F.F., Bufalini, J.J., 1993. Comparison of chemiluminescence and ultraviolet ozone monitor responses in the presence of humidity and photochemical pollutants. Air Waste 43:213–222. https://doi.org/10.1080/1073161X.1993.10467128.

Landis, M.S., Norris, G.A., Williams, R.W., Weinstein, J.P., 2001. Personal exposures to PM2.5 mass and trace elements in Baltimore, MD, USA. Atmos. Environ. 35: 6511–6524. https://doi.org/10.1016/S1352-2310(01)00407-1.

Landis, M.S., Pancras, J.P., Graney, J.R., Stevens, R.K., Percy, K.E., Krupa, S., 2012. Receptor modeling of epiphytic lichens to elucidate the sources and spatial distribution of inorganic air pollution in the Athabasca Oil Sands Region. In: Percy, K.E. (Ed.), Alberta Oil Sands: Energy, Industry and the Environment. Elsevier, Oxford, England, p. 427.

Landis, M.S., Pancras, J.P., Graney, J.R., White, E.M., Edgerton, E.S., Legge, A., Percy, K.E., 2017. Source apportionment of ambient fine and coarse particulate matter at the Fort McKay community site, in the Athabasca Oil Sands Region, Alberta, Canada. Sci. Total Environ. 584–585:105–117. https://doi.org/10.1016/j.scitotenv.2017.01.110.

Lee, G.E., Breysse, P.N., McDermott, A., Eftim, S.E., Geyh, A., Berman, J.D., Curriero, F.C., 2014. 2014 Canadian forest fires and the effects of long-range transboundary air pollution on hospitalization among the elderly. ISPRS Int. Journal of Geo-Inf. 3 (2): 713–731. https://doi.org/10.3390/ijgi3020713.

Littell, J.S., McKenzie, D., Peterson, D.L., Westerling, A.L., 2009. Climate and wildfire area burned in western U. S. ecoprovinces, 1916–2003. Ecol. Appl. 19:1003–1021. https://doi.org/10.1890/07-1183.1.

Liu, J.C., Pereira, G., Uhl, S.A., Bravo, M.A., Bell, M.L., 2015. A systematic review of the physical health impacts from non-occupational exposure to wildfire smoke. Environ. Res. 136:120–132. https://doi.org/10.1016/j.envres.2014.10.015.

Liu, X., Huey, L.G., Yokelson, R.J., Selimovic, V., Simpson, I.J., Müller, M., Jimenez, J.L., Campuzano-Jost, P., Beyersdorf, A.J., Blake, D.R., Butterfield, Z., Choi, Y., Crounse, J.D., Day, D.A., Diskin, G.S., Dubey, M.K., Fortner, E., Hanisco, T.F., Hu, W., King, L.E., Kleinman, L., Meinardi, S., Mikoviny, T., Onasch, T.B., Palm, B.B., Peischl, J., Pollack, I.B., Ryerson, T.B., Sachse, G.W., Sedlacek, A.J., Shilling, J.E., Springston, S., St. Clair, J.M., Tanner, D.J., Teng, A.P., Wennberg, P.O., Wisthaler, A., Wolfe, G.M., 2017. Airborne measurements of western U.S. wildfire emissions: Comparison with prescribed burning and air quality implications. J. Geophys. Res.-Atmos. 122:6108–6129. https://doi.org/10.1002/2016JD026315.

Miller, J., Safford, H., Crimmins, M., Thode, A., 2009. Quantitative evidence for increasing forest fire severity in the Sierra Nevada and Southern Cascade Mountains, California and Nevada, USA. Ecosystems 12:16–32. https://doi.org/10.1007/s10021-008-9201-9.

Miranda, A.I., Martins, V., Cascão, P., Amorim, J.H., Valente, J., Tavares, R., Borrego, C., Tchepel, O., Ferreira, A.J., Cordeiro, C.R., Viegas, D.X., Ribeiro, L.M., Pita, L.P., 2010. Monitoring of firefighters exposure to smoke during fire experiments in Portugal. Environ. Int. 36:736–745. https://doi.org/10.1016/j.envint.2010.05.009.

Naeher, L.P., Achtemeier, G.L., Glitzenstein, J.S., Streng, D.R., MacIntosh, D., 2006. Real-time and time-integrated PM2.5 and CO from prescribed burns in chipped and non-chipped plots: firefighter and community exposure and health implications. J. Expo. Sci. Environ. Epidemiol. 16 (4):351–361. https://doi.org/10.1038/sj.jes.7500497.

Nance, J.D., Hobbs, P.V., Radke, L.F., Ward, D.E., 1993. Airborne measurements of gases and particles from an Alaskan Wildfire. J. Geophys. Res. 98:14873–14882. https://doi.org/10.1029/93JD01196.

Natural Resources Canada, 2017. 8 Facts about Canada's boreal forest. Last accessed October 18, 2017. www.nrcan.gc.ca/forests/boreal/17394.

Ortega, A.M., Day, D.A., Cubison, M.J., Brune, W.H., Bon, D., de Gouw, J.A., Jimenez, J.L., 2013. Secondary organic aerosol formation and primary organic aerosol oxidation from biomass-burning smoke in a flow reactor during FLAME-3. Atmos. Chem. Phys. 13:11551–11571. https://doi.org/10.5194/acp-13-11551-2013.

O'Shea, S.J., Allen, G., Gallagher, M.W., Bauguitte, S.J.-B., Illingworth, S.M., Le Breton, M., Muller, J.B.A., Percival, C.J., Archibald, A.T., Oram, D.E., Parrington, M., Palmer, P.I., Lewis, A.C., 2013. Airborne observations of trace gases over boreal Canada during BORTAS: campaign climatology, air mass analysis and enhancement ratios. Atmos. Chem. Phys. 13:12451–12467. https://doi.org/10.5194/acp-13-12451-2013.

Percy, K.E., 2013. Ambient air quality and linkage to ecosystems in the Athabasca Oil Sands, Alberta. Geosci. Can. 40:182–201. https://doi.org/10.12789/geocanj.2013.40.014.

Phillips-Smith, C., Jeong, C.-H., Healy, R.M., Daebk-Zlotorzynska, E., Celo, V., Brook, J.R., Evans, G., 2017. Sources of particulate matter in the Athabasca Oil Sands Region: investigation through a comparison of trace element measurement methodologies. Atmos. Chem. Phys. Discuss. https://doi.org/10.5194/acp-2016-966 (in review).

Reid, C.E., Brauer, M., Johnson, F.H., Jerrett, J., Balmes, J.R., Elliott, C.T., 2016. Critical review of health impacts of wildfire smoke exposure. Environ. Health Perspect. 124: 1334–1343. https://doi.org/10.1289/ehp.1409277.

Saarnio, K., Aurela, M., Timonen, H., Saarikoski, S., Teinila, K., Makela, T., Sofiev, M., Koskinen, J., Aalto, P.P., Kulmala, M., Kukkonen, J., Hillamo, R., 2010. Chemical composition of fine particles in fresh smoke plumes from boreal wild-land fires in Europe. Sci. Total Environ. 408:2527–2542. https://doi.org/10.1016/j.scitotenv.2005.01.024.

Schweizer, D., Cisneros, R., Shaw, G., 2016. A comparative analysis of temporary and permanent beta attenuation monitors: the importance of understanding data and equipment limitations when creating PM2.5 air quality health advisories. Atmos. Pollut. Res. 7:865–875. https://doi.org/10.1016/j.apr.2016.02.003.

Simpson, I.J., Akagi, S.K., Barletta, B., Blake, N.J., Choi, Y., Diskin, G.S., Fried, A., Fuelberg, H.E., Meinardi, S., Rowland, F.S., Vay, S.A., Weinheimer, A.J., Wennberg, P.O., Wiebring, P., Wisthaler, A., Yang, M., Yokelson, R.J., Blake, D.R., 2011. Boreal forest fire emissions in fresh Canadian smoke plumes: C1–C10 volatile organic compounds (VOCs), CO2, CO, NO2, NO, HCN and CH3CN. Atmos. Chem. Phys. 11:6445–6463. https://doi.org/10.5194/acp-11-6445-2011.

Singh, H.B., Anderson, B.E., Brune, W.H., Cai, C., Cohen, R.C., Crawford, J.H., Cubison, M.J., Czech, E.P., Emmons, L., Fuelberg, H.E., Huey, G., Jacob, D.J., Jimenez, J.L., Kaduwela,

A., Kondo, Y., Mao, J., Olson, J.R., Sachse, G.W., Vay, S.A., Weinheimer, A., Wennberg, P.O., Wisthaler, A., 2010. Pollution influences on atmospheric composition and chemistry at high northern latitudes: boreal and California forest fire emissions. Atmos. Environ. 44:4553–4564. https://doi.org/10.1016/j.atmosenv.2010.08.026.

Spicer, C.W., Joseph, D.W., Ollison, W.M., 2010. A re-examination of ambient air ozone monitor interferences. J. Air Waste Manag. Assoc. 60:1353–1364. https://doi.org/10.3155/1047-3289.60.11.1353.

Stocks, B.J., Mason, J.A., Todd, J.B., Bosch, E.M., Wotton, B.M., Amiro, B.D., Flannigan, M.D., Hirsch, K.G., Logan, K.A., Martell, D.L., Skinner, W.R., 2003. Large forest fires in Canada, 1959–1997. J. Geophys. Res. 108, D08149. https://doi.org/10.1029/2001JD000484.

Sullivan, A.P., Frank, N., Kenski, D.M., Collett Jr., J.L., 2011a. Application of high-performance anion-exchange chromatography – pulsed amperometric detection for measuring carbohydrates in routine daily filter samples collected by a national network: 2. Examination of sugar alcohols/polyols, sugars, and anhydrosugars in the upper Midwest. J. Geophys. Res. 116, D08303. https://doi.org/10.1029/2010JD014169.

Sullivan, A.P., Frank, N., Onstad, G., Simpson, C.D., Collett Jr., J.L., 2011b. Application of high-performance anion-exchange chromatography - pulsed amperometric detection for measuring carbohydrates in routine daily filter samples collected by a national network: 1. Determination of the impact of biomass burning in the Upper Midwest. J. Geophys. Res. 116, D08302. https://doi.org/10.1029/2010JD014166.

Sullivan, A.P., May, A.A., Lee, T., McMeeking, G.R., Kreidenweis, S.M., Akagi, S.K., Yokelson, R.J., Urbanski, S.P., Collett Jr., J.L., 2014. Airborne-based source smoke marker ratios from prescribed burning. Atmos. Chem. Phys. 14:10535–10545. https://doi.org/10.5194/acp-14-10535-2014.

United Stated National Institute for Occupational Safety and Health, Manual of Analytical Methods (NMAM), O'Connor, P.F., Schlecht, P.C., 2003. Monitoring of Diesel Particulate Exhaust in the Workplace, Chapter Q, Third Supplement to NMAM, 4th Edition, NIOSH, Cincinnati, OH. DHHS (NIOSH) Publication No. 2003-154.

United States Department of Agriculture, 2014. United States Forest Resource Facts and Historical Trends, FS-1035: Washington, DC. https://www.fia.fs.fed.us/library/brochures/docs/2012/ForestFacts_1952-2012_English.pdf.

United States Department of Agriculture, 2016. Forest Health Monitoring: National Status, Trends, and Analysis 2015. Forest Service Research & Development, Southern Research Station, SRS-213, Asheville, NC.

United States Environmental Protection Agency, 1997. Method 300.1 Determination of Inorganic Anions in Drinking Water by Ion Chromatography. http://water.epa.gov/scitech/drinkingwater/labcert/upload/met300.pdf Last accessed September 19, 2017.

United States Environmental Protection Agency, 1999a. Laboratory Study to Explore Potential Interferences to Air Quality Monitors. Office of Air Quality Planning and Standards, EPA-454/C-00-002: Research Triangle Park, NC. https://www3.epa.gov/ttnamti1/archive/files/ambient/criteria/reldocs/finalreport.pdf Last accessed September 19, 2017.

United States Environmental Protection Agency, 1999b. Compendium Method IO-4.2: Determination of Reactive acidic and basic gases and strong acidity of atmospheric fine particles (<2.5 μm). Office of Research and Development, Compendium of Methods for the Determination of Inorganic Compounds in Ambient Air, EPA/625/R-96/010a: Cincinnati, OH. https://www3.epa.gov/ttnamti1/files/ambient/inorganic/mthd-4-2.pdf Last accessed September 19, 2017.

United States Environmental Protection Agency, August, 2015. 2011 National Emissions Inventory (NEI) Technical Support Document, Office of Air Quality Planning and Standards, Research Triangle Park, NC, https://www.epa.gov/sites/production/files/2015-10/documents/nei2011v2_tsd_14aug2015.pdf Last accessed September 19, 2017.

United States Environmental Protection Agency, 2016. Climate Change Indicators in the United States: 2016 Fourth Edition, EPA 430-R-16-004: Washington, DC. https://www.epa.gov/sites/production/files/2016-08/documents/climate_indicators_2016.pdf Last accessed September 19, 2017.

United States Wildland Fire Leadership Council, 2016. Monitoring Trends in Burn Severity (MTBS) Project Database. Last accessed September 19, 2017. http://mtbs.gov/dataaccess.html.

United States National Interagency Fire Center, 2017. Historical Wildland Fire Information. Last accessed October 18. https://www.nifc.gov/fireInfo/fireInfo_statistics.html.

Urbanski, S.P., 2013. Combustion efficiency and emission factors for wildfire-season fires in mixed conifer forests of the northern Rocky Mountains, US. Atmos. Chem. Phys. 13: 7241–7262. https://doi.org/10.5194/acp-13-7241-2013.

Weakley, A.T., Takahama, S., Dillner, A.M., 2016. Ambient aerosol composition by infrared spectroscopy and partial least-squares in the chemical speciation network: Organic carbon with functional group identification. Aerosp. Sci. Technol.:1096–1111 https://doi.org/10.1080/02786826.2016.1217389.

Westerling, A.L., 2016. Increasing western U.S. forest wildfire activity: Sensitivity to changes in the timing of spring. Philos. Trans. R. Soc. B 371. https://doi.org/10.1098/rstb.20150178.

Wood Buffalo Environmental Association (WBEA), 2016. Annual Report – Volume I Continuous Monitoring, March 17. Wbea.org/resources/reports-and-publications/ambient-air-monitoring-reports/ambient-annual-report Last accessed September 19, 2017.

Worden, H., Beer, R., Rinsland, C.P., 1997. Airborne infrared spectroscopy of 1994 western wildfires. J. Geophys. Res. 102:1297–1299. https://doi.org/10.1029/96JD02982.

Yokelson, R.J., Goode, J.G., Ward, D.E., Susott, R.A., Babbitt, R.E., Wade, D.D., Bertschi, I., Griffith, D.W.T., Hao, W.M., 1999. Emissions of formaldehyde, acetic acid, methanol, and other trace gases from biomass fires in North Carolina measured by airborne Fourier transform infrared spectroscopy. J. Geophys. Res. 104:30109–30125. https://doi.org/10.1029/1999JD900817.

Yokelson, R.J., Crounse, J.D., DeCarlo, P.F., Karl, T., Urbanski, S., Atlas, E., Campos, T., Shinozuka, Y., Kapustin, V., Clarke, A.D., Weinheimer, A., Knapp, D.J., Montzka, D.D., Holloway, J., Weibring, P., Flocke, F., Zheng, W., Toohey, D., Wennberg, P.O., Wiedinmyer, C., Mauldin, L., Fried, A., Richter, D., Walega, J., Jimenez, J.L., Adachi, K., Buseck, P.R., Hall, S.R., Shetter, R., 2009. Emissions from biomass burning in the Yucatan. Atmos. Chem. Phys. 9:5785–5812. https://doi.org/10.5194/acp-9-5785-2009.